Estimation of Site Response and Qs Factor in the Khorasan Seismic Network Using Inversion Method

A. Zarean[1], H. Sadeghi[2], and E. Haghshenas[3]

1. MSc. Student, Earthquake Research Center, Ferdowsi University, Mashhad, I.R. Iran, email: ahmad19091909@yahoo.com
2. Assistant Professor, Earthquake Research Center, Ferdowsi University, Mashhad, I.R. Iran
3. Assistant Professor, Geotechnical Research Center, International Institute of Earthquake Engineering and Seismology (IIEES), Tehran, I.R. Iran

ABSTRACT: *Site amplification in the Khorasan Seismic Network, Iran, was estimated using small earthquake events (ML 1.6-5.5) recorded from 2003 to 2006. This seismic network consists of 5 broad band stations (NJ, MH, BJ, QU and SB) distributed in Razavi and North Khorasan provinces. A total of 255 three-component waveforms from 88 events were used in this study. The wide dynamic range of the Guralp instrument provided a broadband seismogram for S-waves. Site effects were estimated by linear inversion using the reference site (NJ). The S-wave quality factor was found to be approximated by the relation* $165f^{0.48}$ *in the frequency range 0.6-10Hz. It was found that the site-amplification factor for three kinds of geometrical spreading model* R^{-1}, $R^{-0.75}$, $R^{-0.5}$ *was similar but the quality factor varied.*

Keywords: Site effect; Spectral ratio; Inversion; Khorasan

1. Introduction

The assessment of local site effects on seismic ground motions is of great significance in earthquake engineering research and applications. Several destructive earthquakes, such as the Loma Prieta earthquake in California in October1989, the Northridge earthquake in California in January 1994, the Kobe earthquake in Japan in January 1995, and the western Tottori earthquake in Japan in October 2000, have demonstrated that the amplification of ground motion and associated damage to structures due to local site conditions is a very important consideration in seismic hazard analysis. The role of surface geology in seismic motions is important for both seismic hazard mitigation and detailed analyses of earthquake source characteristics. In fact, the accurate estimation of earthquake source parameters can not be achieved without proper understanding of the local site and path effects. Ground motions in the frequency range of 0.5-10Hz, which are of most engineering interest, are strongly affected by local site conditions, such as complex surface geology and irregular topography. Several analytical and experimental approaches have been developed for local site effect estimation. The most common experimental approach is the direct spectral ratio method [3]. This approach is based on removing the source and path effects. This technique takes into account the ratio between the spectrum at a site of interest and the spectrum at a reference site, which is usually a nearby rock site. If the two sites have similar source and path effects, then the resulting spectral ratio constitutes an estimate of site amplification. The spectral ratio method, however, depends on the availability of a proper reference site for which amplification is negligible. The critical assumption in this method is that the record of a surface reference rock site is equivalent to the input motion at the base of the soil layer. However, a number of studies have revealed significant variability in surface ground motions over even small distances at both soil and rock sites [6]. This variability, particularly at rock sites, suggests that this basic assumption of equivalent motion may not hold above

a site dependent frequency [6]. Furthermore, from comparisons of ground motions recorded simultaneously at the surface and in boreholes, Steidl et al [6] showed that surface rock sites can exhibit anomalous site responses, which can lead to an underestimation of the seismic hazard if such sites are used as reference.

The method of spectral ratio was recast by Andrews [1] into a generalized-inverse problem so that source, path, and site effects are all obtained using earthquake motions recorded at many sites during various kinds of earthquakes. Many other researchers have since applied various forms of this generalized inversion scheme [2, 4], however, there is one undetermined degree of freedom and trade-off problems in the formulation of the generalized inversion.

Small events recorded during 2003 to 2006 observed at Khorasan Seismic Network stations allowed us to study site response on S-waves. With the high dynamic range and broad frequency response of the Guralp instruments, the complete waveforms of the S-waves was obtained. Using the seismograms observed at five Guralp stations, S-wave site-amplification factors were evaluated using a linear inversion method on the direct S-wave portion of data set [1].

2. Data

Three-component waveforms recorded at five stations (*NJ, MH, BJ, QU,* and *SB*) of the Khorasan array were collected. All stations were equipped with a broadband Guralp seismometer and Quanterra data logger with a 24-bit digitizer at 25 *samples/sec.* The gain of a Guralp instrument is constant to ground velocity between 0.0027 and 100*Hz.*

255 waveforms were analyzed from 88 small events at Khorasan Seismic Network stations. These events occurred from January 2003 to December 2006 with a range of magnitudes from 1.6 to 5.5 and a focal depth of less than 16*km.* The epicentral distances ranged from 32 to 210*km.* Station *NJ* is located on Rock, whereas stations *BJ, MH, SB,* and *QU* are on different kinds of soil that are not known perfectly. Subsurface structure and near-surface velocity are uncertain, and only geological information such as rock types is available at each station. Figure (1) shows a distribution of stations. The horizontal seismograms were rotated into radial and transverse components with respect to their azimuth to the epicenter. Figure (2) shows examples of three-component velocity seismograms observed at *NJ.* Fourier amplitudes of

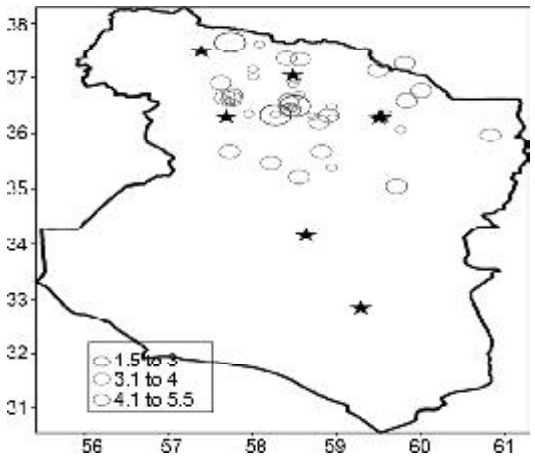

Figure 1. Locations of Khorasan Seismic Network stations and the events have been used.

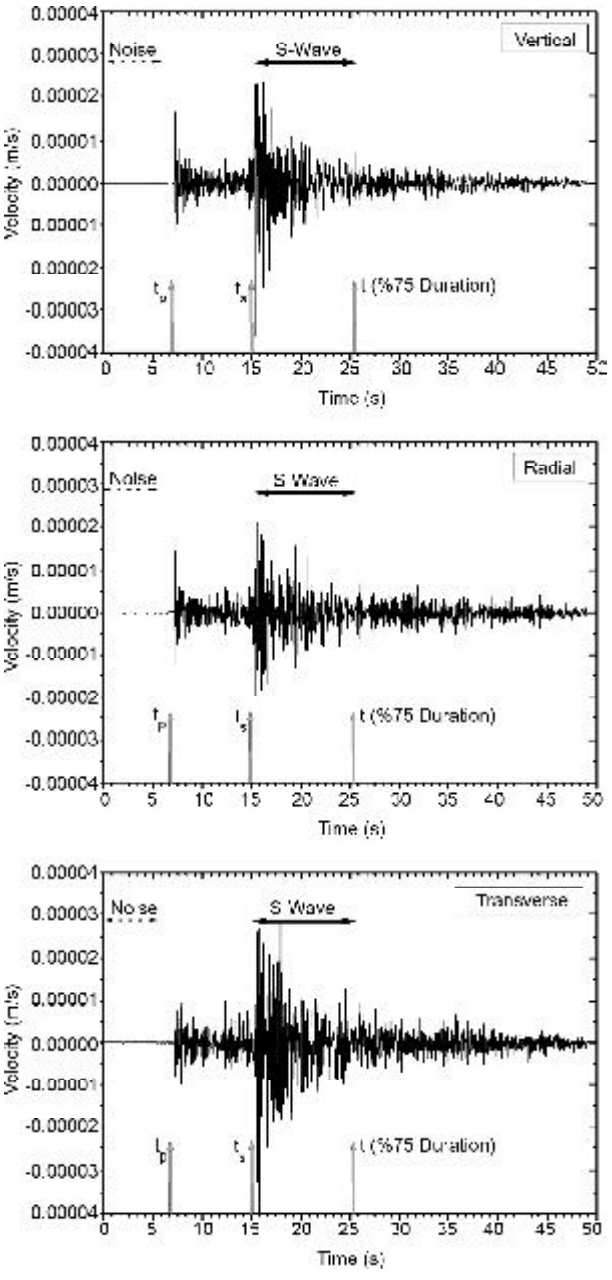

Figure 2. Examples of three-component particle-velocity seismograms observed at NJ.

S-waves were computed using the *FFT* for the records of each station. We first visually determined the onset times of S-waves on the seismograms, indicated by the vertical arrows in Figure (2). Then the S-wave trains were extracted with a cosine-tapered window. The window length was determined using computation of the 75 percent signal duration. Figure (3) shows an example of Fourier amplitudes for S-waves selected windows (solid lines) and noise window (dash lines). Fourier amplitudes for S-waves selected windows were averaged over frequency bands centered at 0.6, 0.7, 0.8, 0.9, 1.0, 1.2, 1.4, 1.6, 1.8, 2.0, 2.2, 2.4, 2.6, 2.8, 3.0, 3.2, 3.4, 3.6, 3.8, 4.0, 4.4, 4.8, 5.2, 5.6, 6.0, 6.4, 6.8, 7.2, 7.6, 8.0, 8.4, 8.8, 9.2, 9.6, and 10.0*Hz*, in order to get a stable estimate of the amplitudes at the certain frequencies. Frequency bandwidths were ±0.1*Hz* for the 0.6 to 1.0*Hz* bands, ±0.2*Hz* for the 1.0 to 4.0*Hz* bands, and ±0.4*Hz* for the remaining center frequencies. A time window in the prevent portion of the records was used to examine the noise level, and only the data with a signal/noise ratio greater than 3 were used in the analysis (The dashed lines in Figure (3) show the noise spectrum). The Fourier spectra of the noise sample was calculated, and then averaged over the respective bandwidth. The squared amplitudes of the noise were then subtracted from those of S waves, assuming statistical independence between the noise and signal. The distance calculated from the *S-P* time was used as the hypocentral distance with regard to travel time table of Khorasan. All three radial, transverse and vertical components were analyzed.

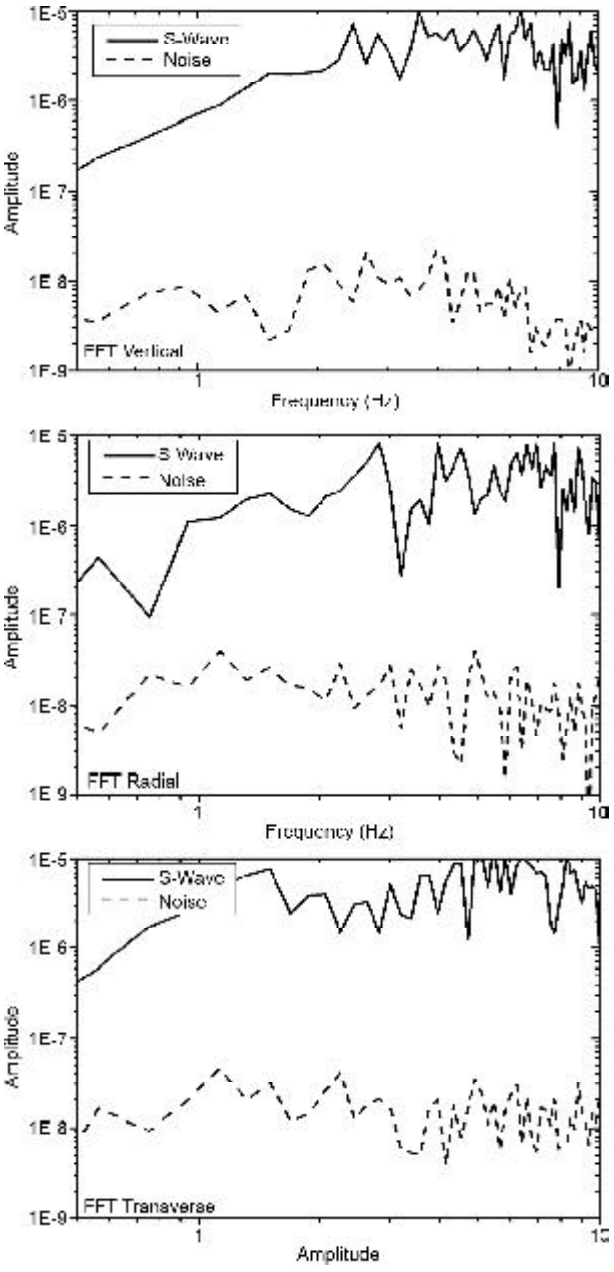

Figure 3. The Fourier amplitude spectra of the seismograms of Figure (2), S-wave (solid lines) and noise (dash lines).

3. Methods

Assuming that S-waves are radiated from a point source, the Fourier amplitude spectrum of the observed S-wave can be expressed as follows:

$$O_{ij}(f) = S_i(f) G_{ij}(f) R_{ij}^{-\gamma} exp(-\frac{\pi f R_{ij}}{Q(f) V_s}) \qquad (1)$$

Where $O_{ij}(f)$ is the S-wave Fourier amplitude spectrum of the i^{th} event recorded at the j^{th} station, $S_i(f)$ is the source term for the i^{th} event, $G_{ij}(f)$ and R_{ij} are the site term and the hypocentral distance for the i^{th} event and the j^{th} station, respectively. γ is the geometrical spreading, $Q_s(f)$ and *vs* denote the average quality factor and the average velocity of the S-waves in the medium, respectively. Regarding the vast variety of epicentral azimuth, the site effect for the studied sites can be assumed to be independent of the azimuth of the incoming seismic signal and the incidence angle of the S-wave to the station by averaging the results over many earthquakes. In this case, the result of linear inversion using many earthquakes is expected to give the average of site effect over many earthquakes. In Eq. (2), therefore, $G_{ij}(f)$ can be expressed as $G_j(f)$, and Eq. (1) can be rewritten as follows [2, 4]:

$$O_{ij}(f) = S_i(f) G_j(f) R_{ij}^{-\gamma} exp(-\frac{\pi f R_{ij}}{Q(f) V_s}) \qquad (2)$$

The spectral ratio between j^{th} station and the reference station is obtained by:

$$\frac{O_{ij}(f)}{O_{ir}(f)} = \frac{G_j(f)R_{ij}^{-\gamma}exp(-\frac{\pi f R_{ij}}{Q(f)V_s})}{G_r(f)R_{ir}^{-\gamma}exp(-\frac{\pi f R_{ir}}{Q(f)V_s})} \quad (3)$$

Where the subscript "*r*" denotes the reference station by taking the logarithm, Eq. (3) can be rewritten at a fixed frequency as:

$$g_j + \pi f(R_{ir} - R_{ij})/Q(f)V_s = r_{ij} + o_{ij} \quad (4)$$

Here, $g_i = ln\frac{G_j(f)}{G_r(f)}$, $o_{ij} = ln\frac{O_{ij}(f)}{O_{ir}(f)}$, $r_{ij} = \gamma ln\frac{R_{ij}(f)}{R_{ir}(f)}$

Denoting $\alpha_{ij} = \pi f(R_{ir} - R_{ij})/Q(f)V_s$ and $d_{ij} = r_{ij} + o_{ij}$ Eq. (4) becomes:

$$g_j + Q(f)^{-1} = d_{ij} \quad (5)$$

For all events and all stations, Eq. (5) can be expressed in matrix form by:

$$Gm = d \quad (6)$$

Where m is a vector in the model space, d is a vector in the data space, and G is a matrix relating m to d. Figure (4) illustrates the matrix given in Eq. (6) in detail. The unknown parameters of the model space are the site effect relative to the reference site, g_j, and the reciprocal of the average quality factor of the medium, Q^{-1}, for each frequency. The site effect of the reference station is constrained to 1, that is, $g_r(f) = 0$ or $G_r(f) = 1.0$. The inversion was executed by finding a solution of m that minimized the prediction error, $|Gm - d|^{-2}$. A least-squares solution was obtained using the singular value decomposition method [5]. The standard deviations of the model parameters were estimated from diagonal elements of the covariance matrix [5] according to $[cov\, m] = \sigma_d^2[G^T G]^{-1}$ where σ_d^2 is the variance of the data.

$$\begin{array}{lc} & G \\ \textit{1st Station and Its I Records} & \\ & \\ & \\ & \\ & \\ \textit{Jth Station and Its I Records} & \\ & \\ & \\ & \end{array} \begin{bmatrix} 1\ 0\ 0\ \ldots\ 0\ \alpha_{11} \\ 1\ 0\ 0\ \ldots\ 0\ \alpha_{21} \\ \ldots\ \ldots\ \ldots\ \ldots\ \ldots \\ 1\ 0\ 0\ \ldots\ 0\ \alpha_{I1} \\ \\ \\ \\ 0\ 0\ 0\ \ldots\ 0\ \alpha_{1J} \\ 0\ 0\ 0\ \ldots\ 0\ \alpha_{2J} \\ \ldots\ \ldots\ \ldots\ \ldots\ \ldots \\ 0\ 0\ 0\ \ldots\ 0\ \alpha_{IJ} \end{bmatrix} \begin{Bmatrix} g_1 \\ . \\ . \\ . \\ g_J \\ Q_s^{-1} \end{Bmatrix} = \begin{Bmatrix} d_{11} \\ d_{21} \\ \ldots \\ d_{I1} \\ . \\ . \\ . \\ d_{1J} \\ d_{2J} \\ \ldots \\ d_{IJ} \end{Bmatrix}$$

Figure 4. Details of the matrix given in Eq. (6). The subscripts I and J denote the total number of events and stations, respectively.

4. Results

Figure (5) shows the site amplification factors for all stations except the reference site, using the generalized inversion. In Figure (5), the site amplification factors of all stations are plotted except for the reference site. Solid line represents the amplification for all stations, and the bars denote the standard deviations. In this figure geometrical spreading factor γ is assumed to be 1. We assumed three values of γ, 0.5, 0.75, and 1.0, because observations show γ deviates from 1.0 due to, for instance, the Moho post critical reflection. Then the linear inversion was independently applied for the different γ values, see Figure (6).

The Q^{-1} for the vertical, radial and transverse component of the S-waves is plotted in Figure (7), with assuming of $\gamma = 1$. It was found that the S-wave quality factor for horizontal components is approximated by the relation $Q = 165f^{0.48}$ in the frequency range 0.6-10*Hz*. In Figure (8), it has been showing that Q^{-1} increased significantly with decreasing r. This increase is due to the strong trade-off between γ and Q^{-1}. The variation in Q^{-1} suggests that a unique determination of Q^{-1} is difficult unless the correct geometrical spreading can be determined. Figure (6) shows the site-amplification factor of the transverse component at *QU* station for different assumed γ. Unlike Q^{-1}, the site terms were stable even when γ increased from 0.5 to 1.0, supporting the idea that the site terms were isolated from S-wave spectra. This separateness of the site term from the attenuation was confirmed for the vertical, radial, and transverse components as well. In the following analysis, $\gamma = 1$ was used as the geometrical spreading factor. Figure (9) shows the S-wave site-amplification factors of the vertical, radial and transverse components relative to *NJ* for all stations. Each factor was independently determined for each component.

Figure (10) shows the S-wave site-amplification factor for the vertical, radial, and transverse component for *QU* relative to *NJ*. Although the vertical component is amplified in the same manner as the horizontal components, the amplitudes of radial component are more than the other components. The same result was obtained for Q^{-1}, Figure (11). (Vertical Q^{-1} increased in the same order as the horizontal Q^{-1} but the amplitudes of radial component are more than the other components).

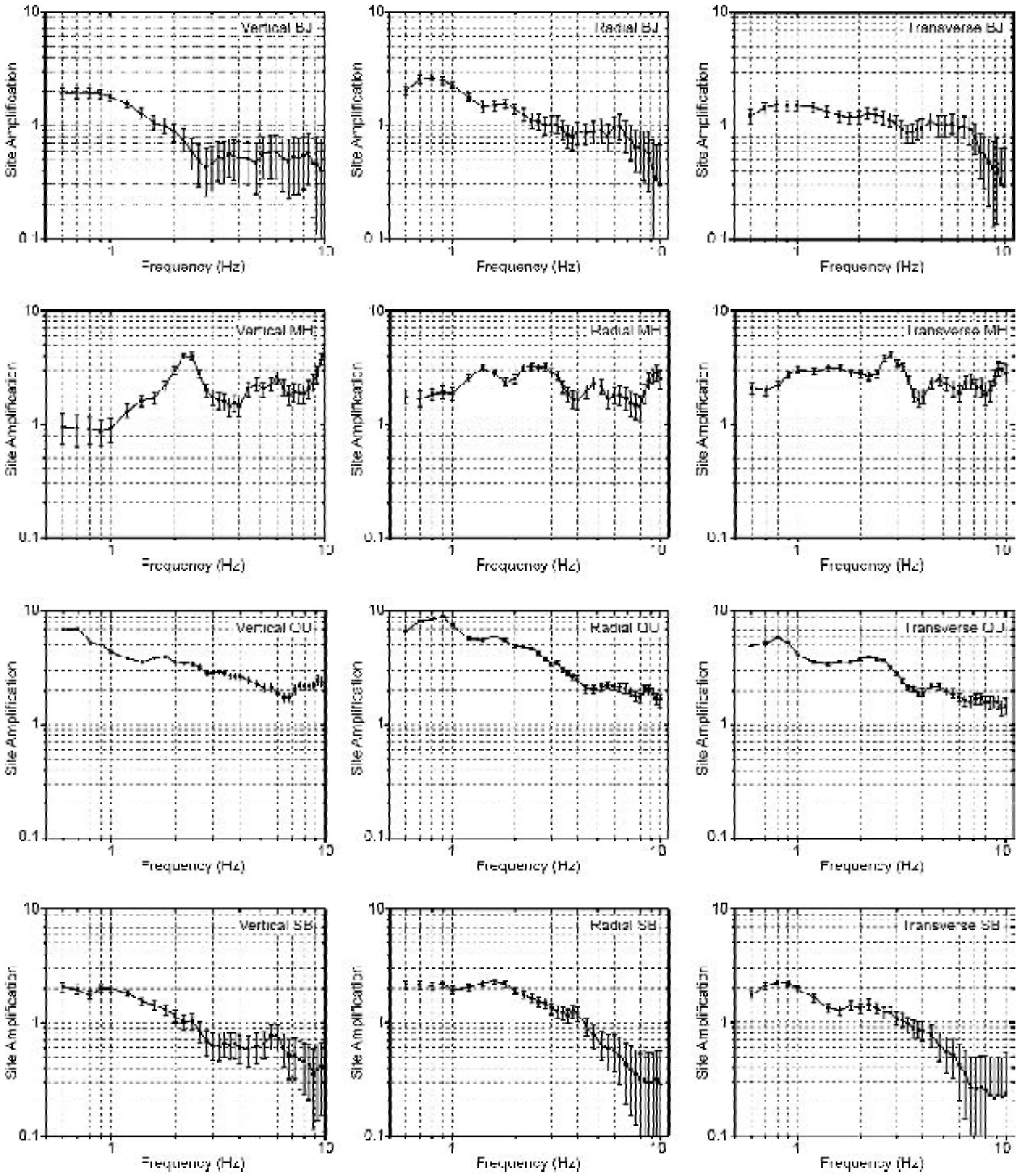

Figure 5. Amplification spectra obtained by the generalized inversion method for all stations except NJ and related standard deviation, left (vertical), middle (radial) and right (transverse).

5. Discussion

In this study, the site amplification was estimated using the generalized inversion method that utilizes the concept of a reference site. This means that the estimated amplifications are relative to that of the selected reference site. Due to the low and moderate size of records that have been used in this study, it is evident that soil deposits would behave linearly.

As described previously, the *NJ* site was designated as reference because it lies on the outcrop consisting of a hard rock. Figure (5) shows that the site amplification factors reached a factor of about 10 at some frequencies, and consistent peaks and troughs are found at each site. It should be noted that the selected reference site may has its own amplifications as opposed to our expectation of flat spectrum with no amplification. Figure (5) shows that the

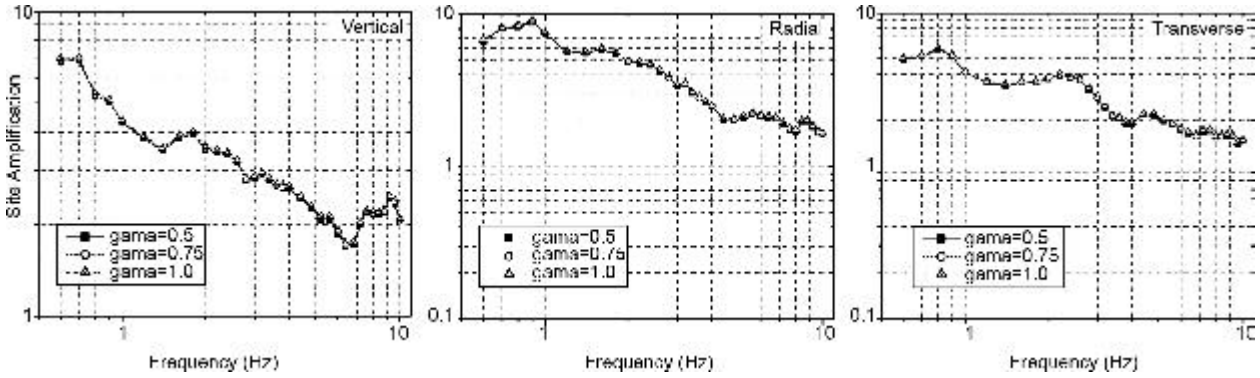

Figure 6. Amplification spectra obtained by the generalized inversion method for QU station and also for three kinds of gamma, left (vertical), middle (radial) and right (transverse).

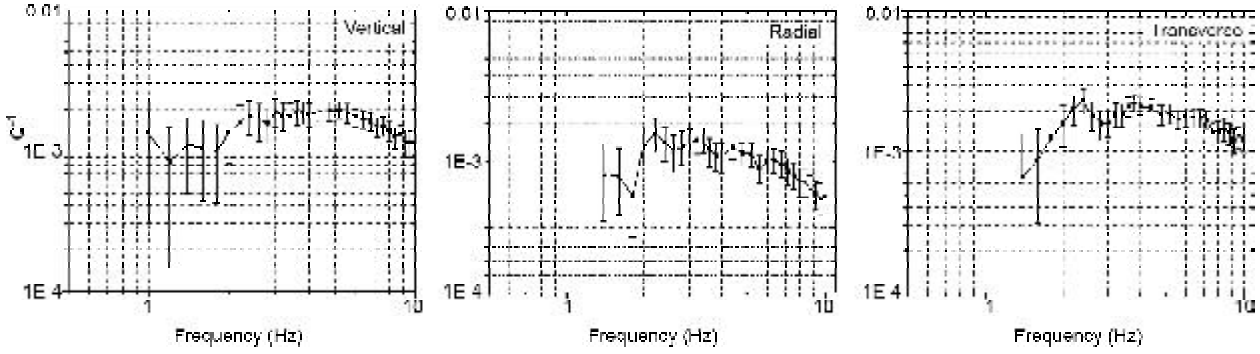

Figure 7. Quality factor obtained by the generalized inversion method for Razavi and north Khorasan, left (vertical), middle (radial) and right (transverse).

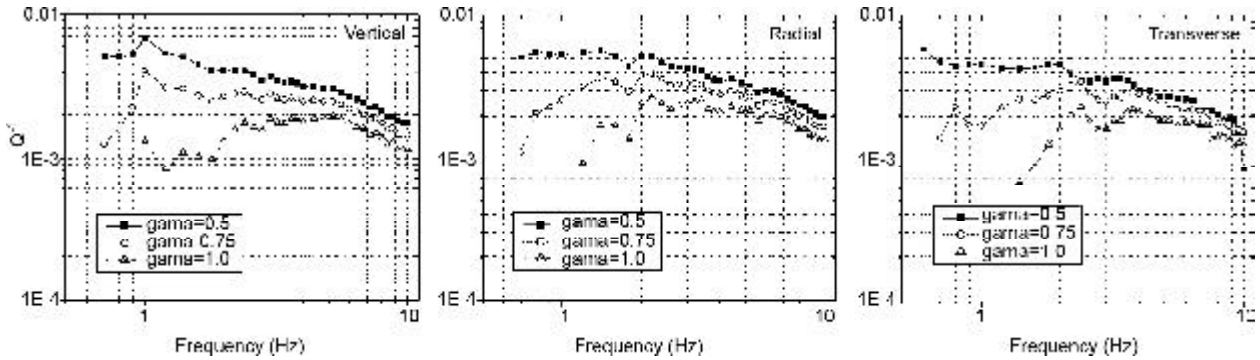

Figure 8. Quality factor obtained by the generalized inversion method for Razavi and north Khorasan and also for three kinds of gamma, left (vertical), middle (radial) and right (transverse).

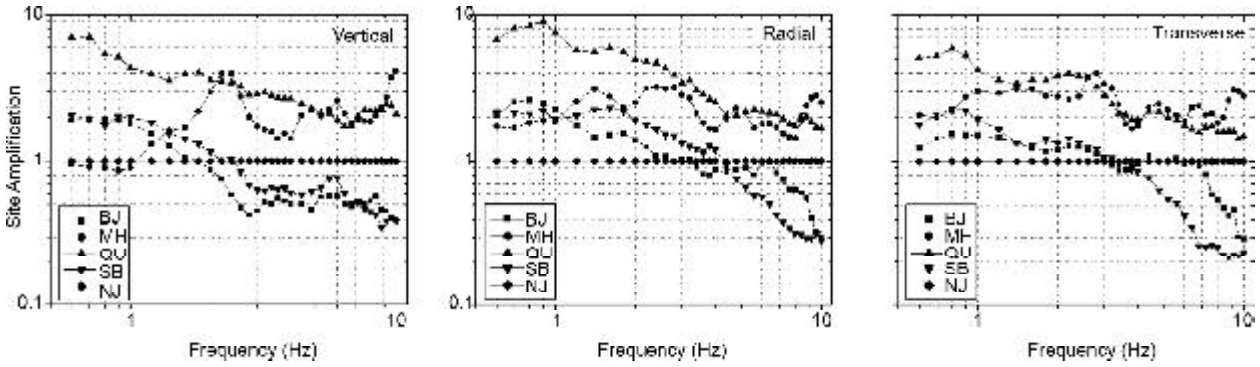

Figure 9. The S-wave site-amplification factors of the (a) vertical, (b) radial, and (c) transverse components relative to NJ for all stations.

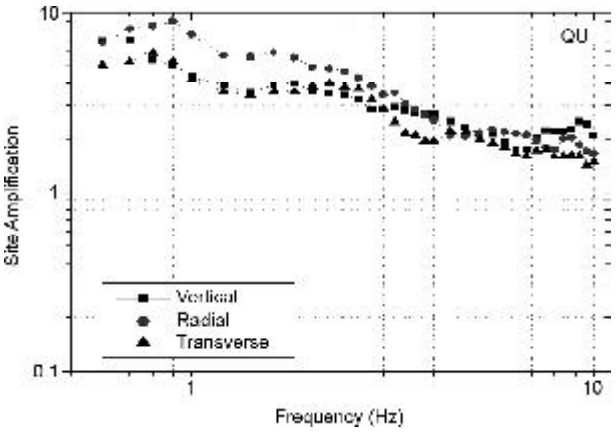

Figure 10. Comparison between site amplification for vertical, radial, and transverse components of Qu.

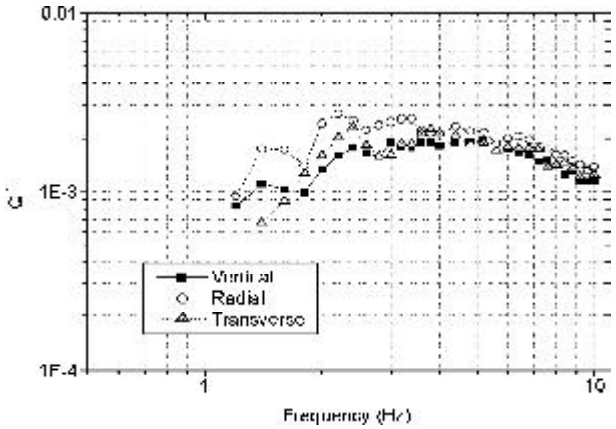

Figure 11. Comparison between Q^{-1} for vertical, radial, and transverse components.

amplification factors vary significantly from one site to another, relating to the effects of soil condition at each site. The amplification factors at site *QU* have a tendency to be greater than the other sites. In addition, predominant frequencies are similar for *QU*, *BJ*, and *SB* (1*Hz* for *QU* station). In contrast, the predominant frequencies of amplification spectra are about 1.5*Hz* and also range from 2.0 to 3.0*Hz* at the site *MH*.

6. Conclusions

S-wave site-amplification factors were evaluated using a total of 255 waveforms from 88 small events recorded at Khorasan Seismic Network stations from 2003 to 2006. The S-wave site-amplification factor was determined using a linear inversion method [1] on the direct S-wave portion of the same data set. Site amplification for *QU* was considerable relative to the other sites especially in low frequencies, and had a pick value on frequency 0.9*Hz* for radial component. Site *MH* had moderate site amplification, and a pick value on frequency 2.4*Hz* for radial component. Two *BJ* and *SB* sites had a little site amplification, and the pick value was in low frequency. It was found that the S-wave quality factor is approximated by the relation $Q = 165f^{0.48}$ in the frequency range 0.6-10*Hz*. Because of a trade-off between Q and geometrical spreading, the accuracy of quality factor can not be confirmed, therefore, Q was evaluated with respect to geometrical spreading $R^{-0.5}$. The advantages of the inversion method are the low value of standard deviation with respect to the standard spectra ratio method and averaging out the effects of directivity and radiation patterns on site amplification. The separateness of the site term from the attenuation term was confirmed for the vertical, radial, and transverse components as well.

Acknowledgments

The authors would like to thank The Earthquake Research Center, Ferdowsi University of Mashhad for providing the raw seismic data and Mr. Farrokhi for helpful and valuable comments and suggestions.

This study was supported by both the Ferdowsi University of Mashhad and Shooray-e-Shahr Research Center of Mashhad.

References

1. Andrews, D.J. (1986). "Objective Determination of Source Parameters and Similarity of Earthquakes of Different Size in Earthquake Source Mechanics", Das, S., Boatwright, J., and Scholz, C.H. (Editors), American Geophysical Union, Washington, DC., 259-268.

2. Boatwright, J., Fletcher, J.B., and Fumal, T.E. (1991). "A General Inversion Scheme for Source, Site, and Propagation Characteristics Using Multiply Recorded Sets of Moderate-Sized Earthquakes", Bull. Seism. Soc. Am., **81**, 1754-1782.

3. Borcherdt, R.D. (1970). "Effects of Local Geology on Ground Motion Near San Francisco Bay", Bull. Seism. Soc. Am., **60**(1), 29-61.

4. Hartzell, S.H. (1992). "Site Response Estimation from Earthquake Data", Bull. Seism. Soc. Am., **82**, 2308-2327.

5. Menke, W. (1984). "Geophysical Data Analysis: Discrete Inverse Theory", Academic Press, New York.

6. Steidl, J.H., Tumarkin, A.G., and Archuleta, R.J. (1996). "What is a Reference Site?", Bull. Seism. Soc. Am., **86**, 1733-1748.